mathematics

Article

Dynamics and Bifurcations of a Discrete-Time Moran-Ricker Model with a Time Delay

Bo Li [1], Zimeng Yuan [1] and Zohreh Eskandari [2,*]

[1] School of Finance, Anhui University of Finance & Economics, Bengbu 233030, China; libo@aufe.edu.cn (B.L.); yuanzimm@163.com (Z.Y.)
[2] Department of Mathematics, Faculty of Science, Fasa University, Fasa 7461686131, Iran
* Correspondence: z-eskandari@fasau.ac.ir

Abstract: This study investigates the dynamics of limited homogeneous populations based on the Moran-Ricker model with time delay. The delay in density dependence caused the preceding generation to consume fewer resources, leading to a decrease in the required resources. Multimodality is evident in the model. Some insect species can be described by the Moran–Ricker model with a time delay. Bifurcations associated with flipping, doubling, and Neimark–Sacker for codimension-one (codim-1) model can be analyzed using bifurcation theory and the normal form method. We also investigate codimension-two (codim-2) bifurcations corresponding to 1:2, 1:3, and 1:4 resonances. In addition to demonstrating the accuracy of theoretical results, numerical simulations are obtained using bifurcation diagrams and phase portraits.

Keywords: bifurcation; numerical normal form; critical normal form coefficient; Neimark–Sacker; period doubling; strong resonance

MSC: 39A28; 65P30

Citation: Li, B.; Yuan, Z.; Eskandari, Z. Dynamics and Bifurcations of a Discrete-Time Moran-Ricker Model with a Time Delay. *Mathematics* **2023**, *11*, 2446. https://doi.org/10.3390/math11112446

Academic Editors: Davide Valenti and Takashi Suzuki

Received: 24 March 2023
Revised: 18 May 2023
Accepted: 22 May 2023
Published: 25 May 2023

1. Introduction

The study of discrete time models defined by difference equations has become increasingly popular in biological mathematics research, particularly for populations with non-overlapping generations [1–9]. Among the various mathematical models used in population dynamics, the Moran–Ricker model is considered one of the most important for characterizing density dependence in single-species population dynamics. The Moran–Ricker model is often employed to analyze the population dynamics of various species, such as the red king crab off Kodiak Island [10]. In previous works [10,11], the Moran–Ricker model with delay was explored in depth to study its dynamical modes, including the appearance and stability criteria for the two- and three-year cycles. More recently, the Moran–Ricker equation has been used to explain local population models with a fundamental age structure and density-dependent regulation, leading to the discovery of various dynamic modes (stable, periodic, and chaotic) that can coexist under the same conditions [11–15]. Interestingly, these models suggest that a change in the observed dynamic mode could result from a random variation in the current population size. In addition to the red king crab, the Moran–Ricker model was also applied to investigating the dynamics of the Larch bud moth [12–16], revealing its chaotic dynamics behavior with time lag. In this study, we use the inner product approach to compute the critical normal form of two types of one-parameter bifurcations and the generating cases, including the 1:2, 1:3, and 1:4 resonances at fixed points of the model. This work provides a deeper understanding of the dynamics of the Moran–Ricker model, and sheds light on the various dynamic modes that can be observed under different conditions.

Time delay is an important feature in ecological models because it can affect the dynamics of populations and communities over time. In many ecological systems, there are time lags between the occurrence of events and their effects on other variables, such as the response of a population to changes in environmental conditions or the feedback between predator and prey populations. Time delays can arise due to a variety of factors, such as biological processes (e.g., growth and reproduction rates), physical transport processes (e.g., the dispersal of organisms or nutrients), and behavioral interactions (e.g., predator avoidance or prey switching).

The aim of this article is to investigate all of the codim-1 bifurcations of the Moran-Ricker model on the basis of such a time lag as transcritical, period-doubling, and Neimark–Sacker bifurcations, considering different values of model parameters and codim-2 bifurcations, such as resonance 1:2, 1:3, and 1:4, assuming the combination of two parameters. The non-degeneracy of codim-1 and codim-2 bifurcations for the delayed Moran-Ricker model is verified using normal form coefficients in this work. This approach has the advantage of avoiding the direct computation of the central manifold and the conversion of the linear component to the Jordan form, and the complexity of the computations is substantially lower than that of the way of computing the central manifold and converting the linear part into the Jordan form. More information can be found in [17–20]. The rest of this paper is organized as follows. Section 2 presents the necessary conditions for flip bifurcation and Neimark–Sacker bifurcation at the fixed points of a discrete-time Moran-Ricker model with delay. In Section 2, the two parameters in the model were chosen as free parameters to investigate the local dynamics generated by 1:2, 1:3, and 1:4 resonance, and we provide the required conditions for 1:2, 1:3, and 1:4 resonance at the model's fixed points. Section 3 provides numerical analysis to demonstrate the theoretical results, and complicated dynamics are shown. Lastly, in Section 4, the conclusions are outlined.

2. Moran-Ricker Model Based on a Time Delay

In Nedorezov [11], the author proposed the following Moran–Ricker model based on a time delay:

$$x_{n+1} = \alpha\, x_n \,\exp(-x_n - \sigma\, x_{n-1}), \tag{1}$$

To eliminate the delay, we could convert the original one-dimensional delay Model (1) into a two-dimensional model as follows:

$$\begin{cases} x_{n+1} = \alpha\, x_n \,\exp(-x_n - \sigma\, y_n), \\ y_{n+1} = x_n. \end{cases} \tag{2}$$

Model (2) are represented with the map depicted below:

$$\begin{pmatrix} x \\ y \end{pmatrix} \mapsto \mathcal{M}(x, y, \alpha, \sigma) = \begin{pmatrix} \alpha x \exp(-\sigma y - x) \\ x \end{pmatrix}. \tag{3}$$

To obtain the fixed points of Model (3), we solve the following equations:

$$\begin{cases} \alpha x \exp(-\sigma y - x) = x, \\ x = y. \end{cases} \tag{4}$$

The solutions of (4) are:

$$F_0 = (0, 0), \quad F_1 = \left(\frac{\ln(\alpha)}{\sigma + 1}, \frac{\ln(\alpha)}{\sigma + 1} \right).$$

The Jacobian matrix of Map (3) is as follows:

$$\mathcal{A}_1(x,y,\alpha,\sigma) = \begin{pmatrix} -\mathrm{e}^{-\sigma\, y - x}\alpha\,(x-1) & -\alpha\, x\sigma\,\mathrm{e}^{-\sigma\, y - x} \\ 1 & 0 \end{pmatrix}.$$

Map $\mathcal{M}$ can be written as follows:

$$\begin{aligned} \mathcal{M}(\xi,\alpha,\sigma) = {} & \mathcal{A}_1(\xi,\alpha,\sigma)\xi + \mathcal{A}_2(\xi,\xi) \\ & + \mathcal{A}_3(\xi,\xi,\xi) + \mathcal{O}(||\xi||^4), \end{aligned} \tag{5}$$

where $\xi = (x,y)$ and

$$\mathcal{A}_2(\xi,\xi) = \begin{pmatrix} \alpha\, x\mathrm{e}^{-\sigma\, y - x}\left(\sigma^2 y^2 + 2\,\sigma\, xy - 2\,\sigma\, y + x^2 - 2\,x\right) \\ 0 \end{pmatrix},$$

$$\mathcal{A}_3(\xi,\xi,\xi) = \begin{pmatrix} -\alpha\, x\mathrm{e}^{-\sigma\, y - x}\left(\sigma^3 y^3 + 3\,\sigma^2 xy^2 - 3\,\sigma^2 y^2 + 3\,\sigma\, x^2 y - 6\,\sigma\, xy + x^3 - 3\,x^2\right) \\ 0 \end{pmatrix}.$$

2.1. Codimension 1 Bifurcation of F_0

Theorem 1. *F_0 undergoes a transcritical (pitchfork) bifurcation at $\alpha = \alpha^{LP,0} = 1$,*

Proof. It is clear that

$$\mathcal{A}_1\left(0,0,\alpha^{LP},\sigma\right) = \begin{pmatrix} 1 & 0 \\ 1 & 0 \end{pmatrix},$$

has eigenvalues $\lambda_1^{LP,0} = -1$ and $\lambda_2^{LP,0} = 0$. This has a simple eigenvalue $+1$ on the provided unit circle $\lambda_2^{PD} \neq \pm 1$. The central manifold corresponding to

$$\mathcal{M}\left(0,0,\alpha^{LP,0},\sigma\right),$$

is one-dimensional and can be considered as follows:

$$C_{PD}(v) = qv + c_2 v^2 + \mathcal{O}(v^3), \quad c_2 = (c_{21}, c_{22})^T, \tag{6}$$

where

$$\mathcal{A}_1\left(0,0,\alpha^{LP,0},\sigma\right)q = -q, \quad \left(\mathcal{A}_1\left(0,0\alpha^{LP,0},\sigma\right)\right)^T p = -p, \quad \langle p,q\rangle = 1,$$

and

$$q = \begin{pmatrix} 1 \\ 1 \end{pmatrix}, \quad p = \begin{pmatrix} 1 \\ 0 \end{pmatrix}.$$

The restriction of $\mathcal{M}\left(0,0,\alpha^{LP,0},\sigma\right)$ to (7) has the following form:

$$w \mapsto w + \sigma_{LP,0} w^2 + \mathcal{O}(w^3),$$

where

$$\sigma_{LP,0} = -1 - \sigma.$$

The dynamics of the Moran–Ricker model at the fixed point F_0 depend on the $\sigma_{LP,0}$ parameter. If this parameter is non-zero, the fixed point undergoes a transcritical bifurcation. Otherwise, a pitchfork bifurcation occurs. Notably, F_0 remains a fixed point and is stable throughout the bifurcation. For a more comprehensive explanation, we refer the reader to [21,22]. □

Remark 1. *In discrete dynamical systems, a fold bifurcation occurs when the Jacobian matrix evaluated at a fixed point has only a simple eigenvalue of* $+1$ *and no other eigenvalues on the unit circle. In this case, the central manifold of the system corresponding to the map has dimension 1, and the map restricted to this manifold has the following form:*

$$w \mapsto -w + \sigma_{LP,0} w^2 + \mathcal{O}(w^4),$$

where $\sigma_{LP,0}$ *is the critical normal form coefficient of the fold bifurcation determined by non-degeneracy and the scenario of the bifurcation.*

2.2. Codimension 1 Bifurcation of F_1

Theorem 2. F_1 *undergoes a flip bifurcation at* $\alpha = \alpha^{PD} = \mathrm{e}^{-2\frac{\sigma+1}{\sigma-1}}$.

Proof. It is clear that

$$\mathcal{A}_1\left(\frac{\ln(\alpha^{PD})}{\sigma+1}, \frac{\ln(\alpha^{PD})}{\sigma+1}, \alpha^{PD}, \sigma\right) = \begin{pmatrix} \frac{\sigma+1}{\sigma-1} & 2\frac{\sigma}{\sigma-1} \\ 1 & 0 \end{pmatrix},$$

has eigenvalues $\lambda_1^{PD} = -1$ and $\lambda_2^{PD} = \frac{2\sigma}{\sigma-1}$. It has a simple eigenvalue -1 on the provided unit circle $\lambda_2^{PD} \neq \pm 1$. The central manifold corresponding to

$$\mathcal{M}\left(\frac{\ln(\alpha^{PD})}{\sigma+1}, \frac{\ln(\alpha^{PD})}{\sigma+1}, \alpha^{PD}, \sigma\right),$$

is one-dimensional and can be considered as follows:

$$C_{PD}(v) = qv + c_2 v^2 + c_3 v^3 + \mathcal{O}(v^4), \quad c_i = (c_{i1}, c_{i2})^T,\ i = 2, 3, \tag{7}$$

where

$$\mathcal{A}_1\left(\frac{\ln(\alpha^{PD})}{\sigma+1}, \frac{\ln(\alpha^{PD})}{\sigma+1}, \alpha^{PD}, \sigma\right) q = -q, \quad \left(\mathcal{A}_1\left(\frac{\ln(\alpha^{PD})}{\sigma+1}, \frac{\ln(\alpha^{PD})}{\sigma+1}, \alpha^{PD}, \sigma\right)\right)^T p = -p, \quad \langle p, q \rangle = 1,$$

and

$$q = \begin{pmatrix} -1 \\ 1 \end{pmatrix}, \quad p = \begin{pmatrix} -\frac{\sigma-1}{3\sigma-1} \\ 2\frac{\sigma}{3\sigma-1} \end{pmatrix}.$$

The restriction of $\mathcal{M}\left(\frac{\ln(\alpha^{PD})}{\sigma+1}, \frac{\ln(\alpha^{PD})}{\sigma+1}, \alpha^{PD}, \sigma\right)$ to (7) has the following form:

$$w \mapsto -w + \beta_{PD} w^3 + \mathcal{O}(w^4),$$

where

$$\beta_{PD} = \frac{1}{6}\frac{(\sigma-1)(\sigma^2 - 2\sigma + 1)}{3\sigma - 1}.$$

The bifurcation is generic, provided $\beta_{PD} \neq 0$. If $\beta_{PD} > 0$ ($\beta_{PD} < 0$) that the bifurcation is supercritical (subcritical); for more details, see [21,22]. □

Remark 2. *In discrete dynamical systems, a flip bifurcation occurs when the Jacobian matrix evaluated at a fixed point has only a simple eigenvalue of* -1 *and no other eigenvalues on the unit circle. In this case, the central manifold of the system corresponding to the map has dimension 1, and the map restricted to this manifold has the following form:*

$$w \mapsto -w + \beta_{PD} w^3 + \mathcal{O}(w^4),$$

where β_{PD} *is the critical normal form coefficient of the flip bifurcation determined by non-degeneracy and the scenario of the bifurcation.*

This remark provides a brief summary of the key characteristics of flip bifurcation in discrete dynamical systems, including the conditions for its occurrence, the dimensionality of the central manifold, and the form of the map restricted to this manifold. It also introduces the concept of the critical normal form coefficient, which is an important parameter for characterizing the behavior of the system near the bifurcation point.

Theorem 3. F_1 *undergoes a Neimark–Sacker bifurcation at* $\alpha = \alpha^{NS} = \mathrm{e}^{\frac{\sigma+1}{\sigma}}$*, provided that* $\sigma > \frac{1}{3}$*.*

Proof. Clearly,

$$\mathcal{A}_1\left(\frac{\ln(\alpha^{NS})}{\sigma+1}, \frac{\ln(\alpha^{NS})}{\sigma+1}, \alpha^{NS}, \sigma\right) = \begin{pmatrix} \frac{\sigma-1}{\sigma} & -1 \\ 1 & 0 \end{pmatrix},$$

has eigenvalues $\lambda_{1,2}^{NS} = \frac{\pm i\sqrt{3\sigma^2+2\sigma-1}+\sigma-1}{2\sigma}$ that $|\lambda_{1,2}^{NS}| = 1$. As $\sigma > \frac{1}{3}$, the pair of complex conjugate $\lambda_{1,2}^{NS}$ lies on the unit circle. This implies that the condition for Neimark–Sacker bifurcation is fulfilled.

The central manifold corresponding to

$$\mathcal{M}\left(\frac{\ln(\alpha^{NS})}{\sigma+1}, \frac{\ln(\alpha^{NS})}{\sigma+1}, \alpha^{NS}, \sigma\right),$$

is two-dimensional and can be considered as follows:

$$C_{NS}(v, \bar{v}) = vq + \bar{v}\bar{q} + \sum_{2\leq k+l} \frac{1}{(k+l)!} c_{kl}(\beta) v^k \bar{v}^l, \quad v \in \mathbb{C}, \quad c_{kl} \in \mathbb{C}, \tag{8}$$

where

$$\mathcal{A}_1\left(\frac{\ln(\alpha)}{\sigma+1}, \frac{\ln(\alpha)}{\sigma+1}, \alpha^{NS}, \sigma\right) q = \lambda_1^{NS} q, \quad \left(\mathcal{A}_1\left(\frac{\ln(\alpha)}{\sigma+1}, \frac{\ln(\alpha)}{\sigma+1}, \alpha^{NS}, \sigma\right)\right)^T p = \lambda_2^{NS} p, \quad \langle p, q\rangle = 1,$$

and

$$q = \begin{pmatrix} 1/2\, \frac{i\sqrt{3\sigma^2+2\sigma-1}+\sigma-1}{\sigma} \\ 1 \end{pmatrix}, \quad p = \begin{pmatrix} \frac{\sigma\left(i\sqrt{3\sigma^2+2\sigma-1}-\sigma+1\right)}{(i\sigma-i)\sqrt{3\sigma^2+2\sigma-1}+3\sigma^2+2\sigma-1} \\ 2\, \frac{\sigma^2}{(i\sigma-i)\sqrt{3\sigma^2+2\sigma-1}+3\sigma^2+2\sigma-1} \end{pmatrix}.$$

The restriction of $\mathcal{M}\left(\frac{\ln(\alpha^{NS})}{\sigma+1}, \frac{\ln(\alpha^{NS})}{\sigma+1}, \alpha^{NS}, \sigma\right)$ to (8) has the form

$$v \mapsto \lambda_1^{NS} v + \gamma_{NS} v|v|^2 + \mathcal{O}(v^4), \quad v \in \mathbb{C},$$

where

$$\gamma_{NS} = \frac{\gamma_{NS}^1(\sigma)}{\gamma_{NS}^2(\sigma)},$$

with

$$\begin{aligned}\gamma_{NS}^1(\sigma) = &\Big(2\,i\sqrt{3\,\sigma^2+2\,\sigma-1}\sigma^4 - 5\,i\sqrt{3\,\sigma^2+2\,\sigma-1}\sigma^3 - 4\,\sigma^5 - 5\,\sigma^4 + 3\,i\sqrt{3\,\sigma^2+2\,\sigma-1}\sigma + 9\,\sigma^3 \\ &-i\sqrt{3\,\sigma^2+2\,\sigma-1} + \sigma^2 - 4\,\sigma + 1\Big)\sigma\left(i\sqrt{3\,\sigma^2+2\,\sigma-1} + \sigma - 1\right), \\ \gamma_{NS}^2(\sigma) = &\,2\,(2\,\sigma-1)\left(i\sqrt{3\,\sigma^2+2\,\sigma-1}\sigma - i\sqrt{3\,\sigma^2+2\,\sigma-1} - 3\,\sigma^2 - 2\,\sigma + 1\right) \\ &\left(i\sqrt{3\,\sigma^2+2\,\sigma-1}\sigma - i\sqrt{3\,\sigma^2+2\,\sigma-1} - \sigma^2 - 2\,\sigma + 1\right).\end{aligned}$$

The bifurcation is generic, provided $\delta_{NS} \neq 0$, where

$$\delta_{NS} = \Re\left(\lambda_2^{NS}\gamma_{NS}\right).$$

If $\delta_{NS} > 0$ ($\delta_{NS} < 0$) the bifurcation is subcritical (supercritical); for more details, see [23]. □

Remark 3. *In discrete dynamical systems, a Neimark–Sacker bifurcation occurs when the Jacobian matrix evaluated at a fixed point has a simple complex conjugate pair of eigenvalues on the unit circle and no other eigenvalues on the unit circle. In this case, the center manifold of the system corresponding to the map has dimension 2, and the map restricted to this manifold has the form:*

$$v \mapsto \lambda_1^{NS}v + \gamma_{NS}v|v|^2 + \mathcal{O}(v^4), \quad v \in \mathbb{C},$$

where γ_{NS} is the critical normal form coefficient of the Neimark–Sacker bifurcation. The value of $\delta_{NS} = \Re(\lambda_2^{NS}\gamma_{NS})$ determines the non-degeneracy and the scenario of the bifurcation.

This remark provides a concise description of the key features of the Neimark–Sacker bifurcation in discrete dynamical systems, including the conditions for its occurrence, the dimensionality of the central manifold, and the form of the map restricted to this manifold. It also introduces the concept of the first Lyapunov coefficient and the normal form coefficient, which are important parameters for characterizing the behavior of the system near the bifurcation point.

2.3. Codimension 2 Bifurcation of F_1

Theorem 4. *F_1 undergoes a 1:2 resonance bifurcation at*

$$\alpha = \alpha^{R_2} = e^4, \quad \sigma = \sigma^{R_2} = \frac{1}{3}.$$

Proof. Clearly,

$$\mathcal{A}_1\left(\frac{\ln(\alpha^{R_2})}{\sigma^{R_2}+1}, \frac{\ln(\alpha^{R_2})}{\sigma^{R_2}+1}, \alpha^{R_2}, \sigma^{R_2}\right) = \begin{pmatrix} -2 & -1 \\ 1 & 0 \end{pmatrix},$$

has eigenvalues $\lambda_{1,2}^{R_2} = -1$ on the unit circle.

The central manifold corresponding to

$$\mathcal{M}\left(\frac{\ln(\alpha^{R_2})}{\sigma^{R_2}+1}, \frac{\ln(\alpha^{R_2})}{\sigma^{R_2}+1}, \alpha^{R_2}, \sigma^{R_2}\right),$$

is two-dimensional and can be considered as follows:

$$C_{R_2}(v_1, v_2) = v_1 q_0 + v_2 q_1 + \sum_{2 \le j+k \le 3} \frac{1}{j1k!} c_{jk} v_1^j v_2^k, \tag{9}$$

where

$$\begin{aligned}
\mathcal{A}_1\left(\frac{\ln(\alpha^{R_2})}{\sigma^{R_2}+1}, \frac{\ln(\alpha^{R_2})}{\sigma^{R_2}+1}, \alpha^{R_2}, \sigma^{R_2}\right) q_0 &= -q_0, \\
\mathcal{A}_1\left(\frac{\ln(\alpha^{R_2})}{\sigma^{R_2}+1}, \frac{\ln(\alpha^{R_2})}{\sigma^{R_2}+1}, \alpha^{R_2}, \sigma^{R_2}\right) q_1 &= -q_1 + q_0 \\
\left(\mathcal{A}_1\left(\frac{\ln(\alpha^{R_2})}{\sigma^{R_2}+1}, \frac{\ln(\alpha^{R_2})}{\sigma^{R_2}+1}, \alpha^{R_2}, \sigma^{R_2}\right)\right)^T p_0 &= -p_0, \\
\left(\mathcal{A}_1\left(\frac{\ln(\alpha^{R_2})}{\sigma^{R_2}+1}, \frac{\ln(\alpha^{R_2})}{\sigma^{R_2}+1}, \alpha^{R_2}, \sigma^{R_2}\right)\right)^T p_1 &= -p_1 + p_0, \\
\langle p_0, q_1 \rangle = \langle p_1, q_0 \rangle = 1, \quad & \langle p_0, q_0 \rangle = \langle p_1, q_1 \rangle = 0,
\end{aligned}$$

and

$$q_0 = \begin{pmatrix} -1 \\ 1 \end{pmatrix}, \quad q_1 = \begin{pmatrix} 0 \\ 1 \end{pmatrix}, \quad p_0 = \begin{pmatrix} 1 \\ 1 \end{pmatrix}, \quad p_1 = \begin{pmatrix} -1 \\ 0 \end{pmatrix}.$$

The restriction of $\mathcal{M}\left(\frac{\ln(\alpha^{R_2})}{\sigma^{R_2}+1}, \frac{\ln(\alpha^{R_2})}{\sigma^{R_2}+1}, \alpha^{R_2}, \sigma^{R_2}\right)$ to (9) has the following form:

$$\begin{pmatrix} v_1 \\ v_2 \end{pmatrix} \mapsto \begin{pmatrix} -v_1 + v_2 \\ -v_2 + \delta_{R2} v_1^3 + \gamma_{R2} v_1^2 v_2 \end{pmatrix}, \quad v = (v_1, v_2) \in \mathbb{R}^2.$$

where

$$\delta_{R_2} = \frac{-2}{27}, \quad \gamma_{R_2} = \frac{5}{18}.$$

The bifurcation is generic because of $\delta_{R2} \neq 0$ and $\gamma_{R2} \neq -3\delta_{R2}$. □

Remark 4. *In discrete dynamical systems, a 1:2 resonance bifurcation occurs when the Jacobian matrix evaluated at a fixed point has two eigenvalues of -1 on the unit circle and no other eigenvalues on the unit circle. In this case, the central manifold of the system corresponding to the map has dimension 2, and the map restricted to this manifold has the following form:*

$$\begin{pmatrix} v_1 \\ v_2 \end{pmatrix} \mapsto \begin{pmatrix} -v_1 + v_2 \\ -v_2 + \delta_{R2} v_1^3 + \gamma_{R2} v_1^2 v_2 \end{pmatrix}, \quad v = (v_1, v_2) \in \mathbb{R}^2.$$

Here, δ_{R2} and γ_{R2} are the critical normal form coefficients of the 1:2 resonance bifurcation that determine the non-degeneracy and the scenario of the bifurcation.

Theorem 5. *F_1 undergoes a 1:3 resonance bifurcation at*

$$\alpha = \alpha^{R_3} = e^3, \quad \sigma = \sigma^{R_3} = \frac{1}{2}.$$

Proof. Clearly,

$$\mathcal{A}_1\left(\frac{\ln(\alpha^{R_3})}{\sigma^{R_3}+1}, \frac{\ln(\alpha^{R_3})}{\sigma^{R_3}+1}, \alpha^{R_3}, \sigma^{R_3}\right) = \begin{pmatrix} -1 & -1 \\ 1 & 0 \end{pmatrix},$$

has eigenvalues $\lambda_{1,2}^{R_3} = \exp(\frac{2\pi i}{3})$ on the unit circle.

The central manifold corresponding to

$$\mathcal{M}\left(\frac{\ln(\alpha^{R_3})}{\sigma^{R_3}+1}, \frac{\ln(\alpha^{R_3})}{\sigma^{R_3}+1}, \alpha^{R_3}, \sigma^{R_3}\right),$$

is two-dimensional and can be considered as follows:

$$C_{R_3}(v,\bar{v}) = vq + \bar{v}\bar{q} + \sum_{2\le j+k} \frac{1}{j1k!} c_{jk} v^j \bar{v}^k, \quad v \in \mathbb{C}, \tag{10}$$

where

$$\mathcal{A}_1\left(\frac{\ln(\alpha^{R_3})}{\sigma^{R_3}+1}, \frac{\ln(\alpha^{R_3})}{\sigma^{R_3}+1}, \alpha^{R_3}, \sigma^{R_3}\right) q = \exp\left(\frac{2\pi i}{3}\right) q,$$

$$\left(\mathcal{A}_1\left(\frac{\ln(\alpha^{R_3})}{\sigma^{R_3}+1}, \frac{\ln(\alpha^{R_3})}{\sigma^{R_3}+1}, \alpha^{R_3}, \sigma^{R_3}\right)\right)^T p = \exp\left(\frac{-2\pi i}{3}\right) p,$$

$$\langle p, q\rangle = 1,$$

and

$$q = \begin{pmatrix} -1/2 + i/2\sqrt{3} \\ 1 \end{pmatrix}, \quad p = \begin{pmatrix} i/3\sqrt{3} \\ -2\left(i\sqrt{3}-3\right)^{-1} \end{pmatrix}.$$

The restriction of $\mathcal{M}\left(\frac{\ln(\alpha^{R_3})}{\sigma^{R_3}+1}, \frac{\ln(\alpha^{R_3})}{\sigma^{R_3}+1}, \alpha^{R_3}, \sigma^{R_3}\right)$ to (10) has the following form:

$$v \mapsto \exp\left(\frac{2\pi}{3} i\right) v + \beta_{R_3}\bar{v}^2 + \delta_{R_3} v|v|^2 + \mathcal{O}(v^4), \quad v \in \mathbb{C}.$$

where

$$\beta_{R_3} = \frac{-1}{4}, \quad \delta_{R_3} = i/16\sqrt{3} + 3/16.$$

The bifurcation is generic because of $1/3\,\frac{e^{4/3\,i\pi}\delta_{R_3}}{(|\beta_{R_3}|)^2} - 1/3 \neq 0$. □

Remark 5. *In discrete dynamical systems, a 1:3 resonance bifurcation occurs when the Jacobian matrix evaluated at a fixed point has two eigenvalues of* $\exp(\frac{2\pi i}{3})$ *on the unit circle and no other eigenvalues on the unit circle. In this case, the central manifold of the system corresponding to the map has dimension 2, and the map restricted to this manifold has the following form:*

$$v \mapsto \exp\left(\frac{2\pi}{3} i\right) v + \beta_{R_3}\bar{v}^2 + \delta_{R_3} v|v|^2 + \mathcal{O}(v^4), \quad v \in \mathbb{C}.$$

Here, β_{R_3} *and* δ_{R_3} *are the critical normal form coefficients of the 1:3 resonance bifurcation that determine the non-degeneracy and the scenario of the bifurcation:*

Theorem 6. *F_1 undergoes a 1:4 resonance bifurcation at*

$$\alpha = \alpha^{R_4} = e^2, \quad \sigma = \sigma^{R_4} = 1.$$

Proof. Clearly,

$$\mathcal{A}_1\left(\frac{\ln(\alpha^{R_4})}{\sigma^{R_4}+1}, \frac{\ln(\alpha^{R_4})}{\sigma^{R_4}+1}, \alpha^{R_4}, \sigma^{R_4}\right) = \begin{pmatrix} 0 & -1 \\ 1 & 0 \end{pmatrix},$$

has eigenvalues $\lambda_{1,2}^{R_4} = \exp\left(\frac{\pi i}{2}\right)$ on the unit circle.

The central manifold corresponding to

$$\mathcal{M}\left(\frac{\ln(\alpha^{R_4})}{\sigma^{R_4}+1}, \frac{\ln(\alpha^{R_4})}{\sigma^{R_4}+1}, \alpha^{R_4}, \sigma^{R_4}\right),$$

is two-dimensional and can be considered as follows:

$$C_{R_4}(v, \bar{v}) = vq + \bar{v}\bar{q} + \sum_{2 \le j+k} \frac{1}{j1k!} c_{jk} v^j \bar{v}^k, \quad v \in \mathbb{C}, \tag{11}$$

where

$$\mathcal{A}_1\left(\frac{\ln(\alpha^{R_4})}{\sigma^{R_4}+1}, \frac{\ln(\alpha^{R_4})}{\sigma^{R_4}+1}, \alpha^{R_4}, \sigma^{R_4}\right) q = \exp\left(\frac{\pi i}{2}\right) q,$$
$$\left(\mathcal{A}_1\left(\frac{\ln(\alpha^{R_4})}{\sigma^{R_4}+1}, \frac{\ln(\alpha^{R_4})}{\sigma^{R_4}+1}, \alpha^{R_4}, \sigma^{R_4}\right)\right)^T p = \exp\left(\frac{\pi i}{2}\right) p,$$
$$\langle p, q \rangle = 1,$$

and

$$q = \begin{pmatrix} i \\ 1 \end{pmatrix}, \quad p = \begin{pmatrix} \frac{1}{2} i \\ \frac{1}{2} \end{pmatrix}.$$

The restriction of $\mathcal{M}\left(\frac{\ln(\alpha^{R_4})}{\sigma^{R_4}+1}, \frac{\ln(\alpha^{R_4})}{\sigma^{R_4}+1}, \alpha^{R_4}, \sigma^{R_4}\right)$ to (11) has the form

$$v \mapsto \exp\left(\frac{\pi}{2} i\right) v + \delta_{R_4} v^2 \bar{v} + \gamma_{R_4} \bar{v}^3 + \mathcal{O}(v^5), \quad v \in \mathbb{C},$$

where

$$\delta_{R_4} = \frac{1}{4} + \frac{1}{4} i, \quad \gamma_{R_4} = \frac{-1}{12} + \frac{1}{12} i.$$

The bifurcation scenario is determined by

$$A_0^{R_4} = -\frac{i\delta_{R_4}}{|\gamma_{R_4}|}.$$

Since $|A_0^{R_4}| > 1$, there are two limit-point curves of the fourth iteration of $\mathcal{M}\left(\frac{\ln(\alpha^{R_4})}{\sigma^{R_4}+1}, \frac{\ln(\alpha^{R_4})}{\sigma^{R_4}+1}, \alpha^{R_4}, \sigma^{R_4}\right)$. □

Remark 6. *In discrete dynamical systems, a 1:4 resonance bifurcation occurs when the Jacobian matrix evaluated at a fixed point has two eigenvalues of $\pm i$ on the unit circle, and no other eigenvalues on the unit circle. In this case, the central manifold of the system corresponding to the map has dimension 2, and the map restricted to this manifold has the following form:*

$$v \mapsto \exp\left(\frac{\pi}{2}i\right)v + \delta_{R_4}v^2\bar{v} + \gamma_{R_4}\bar{v}^3 + \mathcal{O}(v^5), \quad v \in \mathbb{C},$$

Here, δ_{R_4} and γ_{R_4} are the critical normal form coefficients of the 1:4 resonance bifurcation that determine the non-degeneracy and the scenario of the bifurcation:

3. Numerical Bifurcation Analysis of $\mathcal{M}(x, y, \alpha, \sigma)$

MatContM is a version of MatCont that is specifically designed for the continuation and bifurcation analysis of maps or discrete dynamical systems. It extends the capabilities of MatCont to handle systems that are defined by iterated maps rather than differential equations.

Like MatCont, MatContM is an open-source software package that can be used to analyze a wide range of nonlinear systems. It provides a user-friendly interface for specifying the map, selecting the continuation algorithm, and visualizing the results.

MatContM implements several continuation algorithms that are tailored to the needs of discrete dynamical systems. These include the parameter-homotopy, pseudo-arclength, and tangent-bifurcation methods. It also provides tools for detecting and analyzing various types of bifurcations, including period-doubling, Neimark–Sacker, and saddle-node bifurcations.

One of the strengths of MatContM is its ability to handle systems with multiple parameters and discontinuities. It can also handle systems with higher-dimensional maps, such as those arising in spatially extended systems.

In summary, MatContM is a powerful tool for the continuation and bifurcation analysis of maps or discrete dynamical systems. It is a valuable addition to a toolkit if one is working with discrete dynamical systems, and wants to provide a rigorous and quantitative analysis of their behavior. To confirm the analytical results, we used MATCONTM, which is a toolbox of MATLAB that works on the basis of the numerical continuation method; for more details, see [23,24]. Here, α and σ are considered a free parameter and a fixed parameter, respectively.

We consider two cases for fixed parameter σ.

(i) Case 1: If $0 < \sigma < 1$, we consider $\sigma = 0.1$. With this assumption, a flip bifurcation occurs for $\alpha = 11.524146$ at $F_1 = (2.222222, 2.222222)$ with critical coefficient $\beta_{PD} = 8.678571 \times 10^{-2}$. Because this coefficient is positive, we conclude that the flip bifurcation is supercritical, and the double cycle bifurcated from F_1 is stable. The period doubles when a curve emanates from a PD bifurcation is shown in Figure 1a. A 1:2 resonance bifurcation occurs on the curve of flip bifurcation for $\alpha = 54.598150$ and $\sigma = 0.333333$ at $F_1 = (3.000000, 3.000000)$, see Figure 1b.

(ii) Case 2: If $\sigma > 1$, we consider $\sigma = 1.1$. With this assumption, a Neimark–Sacker bifurcation occurs for $\alpha = 6.746952$ at $F_1 = (0.909091, 0.909091)$ with the first Lyapunov coefficient $\delta_{NS} = -1.512500 \times 10^{-1}$. Since $\delta_{NS} < 0$, we conclude that the Neimark–Sacker bifurcation is supercritical. This phenomenon is shown in Figure 2.

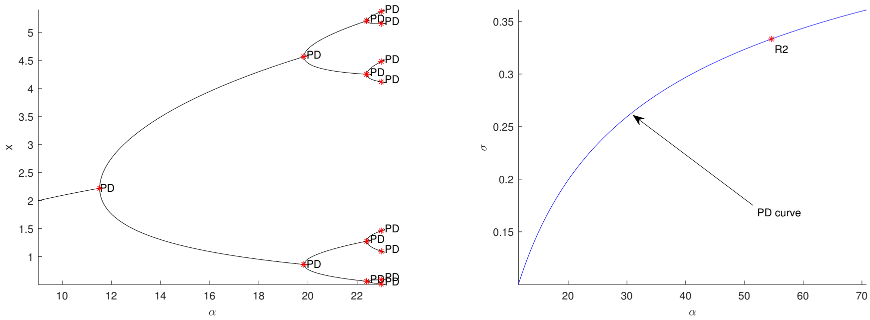

(**a**) (**b**)

Figure 1. Bifurcation diagram of a dynamical system depicting the change in the system's behavior as a parameter is varied. (**a**) Period-doubling cascade in which the system undergoes a series of bifurcations that lead to the emergence of complex dynamics and chaos. (**b**) Curve of flip bifurcation with one codim 2 point that describes the transition from a stable fixed point to a limit cycle as the parameter is varied.

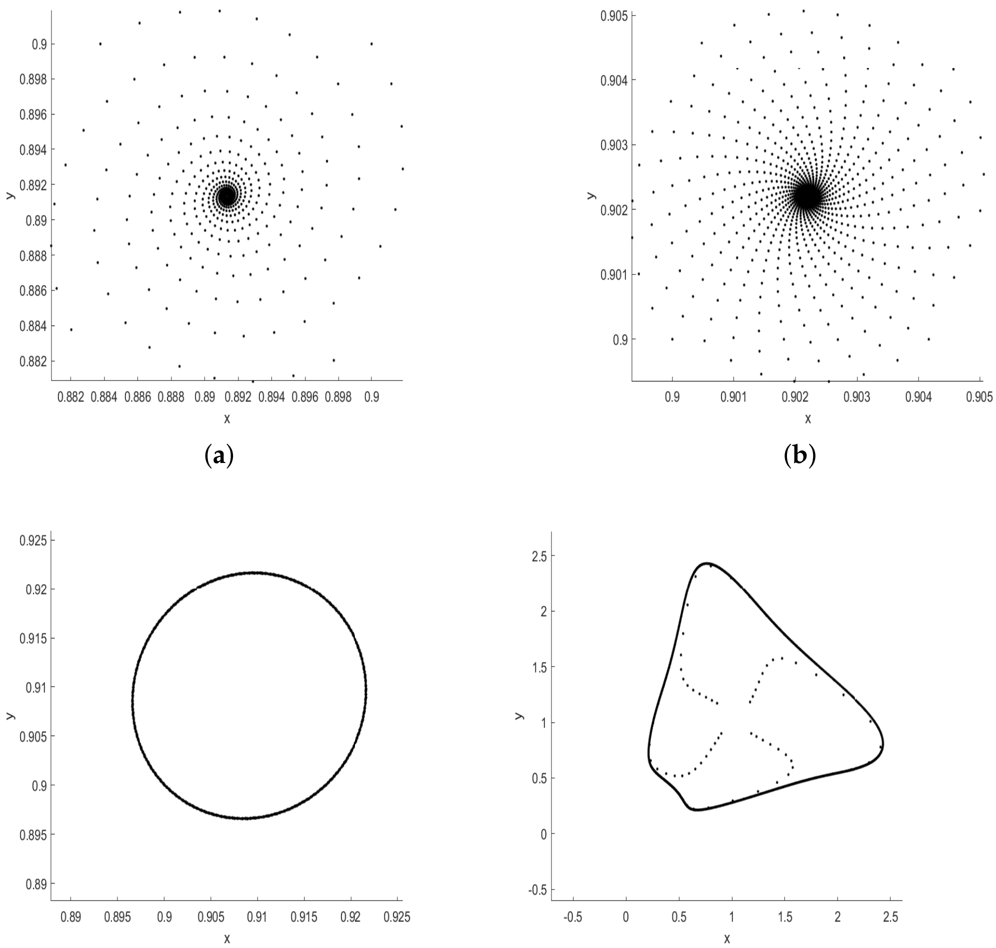

(**a**) (**b**)

(**c**) (**d**)

Figure 2. Phase portraits of $\mathcal{M}(x, y, \alpha, \sigma)$ illustrating the dynamics of the system at different parameter values. (**a**) Stable fixed point for $\alpha = 6.5$ indicating that the system tends to converge to a steady state. (**b**) Closed invariant curve for $\alpha = 6.65$, suggesting the presence of periodic behavior. (**c**) Invariant closed curve for $\alpha = 6.746952$ that exhibits more complex dynamics. (**d**) Broken invariant closed curve for $\alpha = 8.7$, indicating the onset of chaotic behavior in the system.

On the curve, Neimark–Sacker bifurcation caused a 1:4 resonance fifurcation for $\alpha = 7.389056$, $\sigma = 1.000000$ at $F_1 = (1.000000, 1.000000)$ and a 1:3 resonance fifurcation for $\alpha = 20.085537$, $\sigma = 0.500000$ at $F_1 = (2.000000, 2.000000)$, see Figure 3a. The neutral saddle curve of the third iterate $\mathcal{M}(x, y, \alpha, \sigma)$ is presented in Figure 3b.

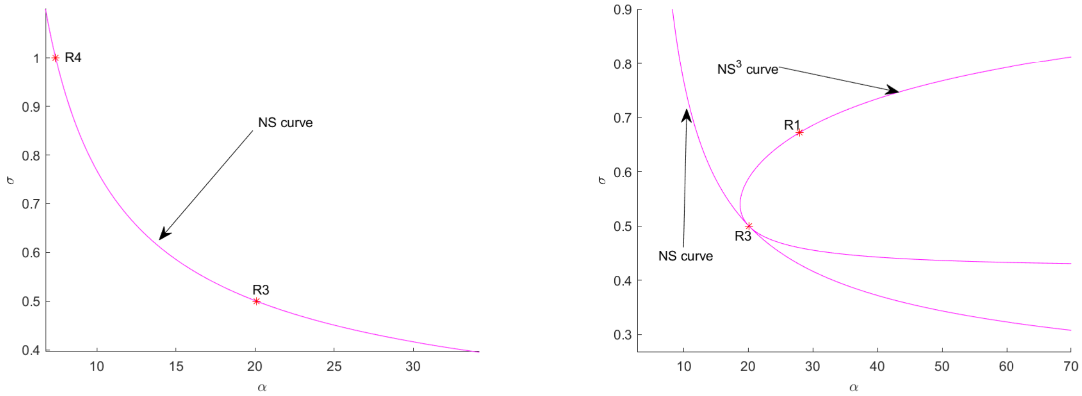

(a) **(b)**

Figure 3. Two curves that describe the behavior of a dynamical system at different parameter values. (**a**) Curve of Neimark–Sacker bifurcation with two codim 2 points that describes the transition from a stable periodic orbit to a chaotic attractor as the parameter is varied. (**b**) Neutral saddle curve of the third iterate of $\mathcal{M}(x, y, \alpha, \sigma)$, which identifies the parameter values where the system exhibits a saddle-node bifurcation, leading to the coexistence of attractors with different basins of attraction.

In the following, the structure of periodic orbits and transitions between them is considered. The 1:4 resonance was set as the initial point, and the corresponding period was computed on a mesh of 1000×1000 parameters (alpha, sigma). Different colors are associated with different periods of the trajectories. It is clear that the stable regions were becoming increasingly smaller as the parameters increased. Almost periodic regions coexist with period-doubling regions. For example, the period-18 and -9 regions. Meanwhile, when compared with Figures 1b and 3a, the Neimark–Sacker bifurcation curve and period-doubling bifurcation curve were also consistent with the border between different types of bifurcations in Figure 4. It is interesting that there existed a series of a period-adding and bar-shaped region with a period higher than four.

Note 1. Please be advised that the following symbols are used in the text:

- PD denotes flip bifurcation.
- NS denotes Neimark–Sacker bifurcation.
- $R2$ denotes 1:2 resonance bifurcation.
- $R3$ denotes 1:3 resonance bifurcation.
- $R3$ denotes 1:4 resonance bifurcation.

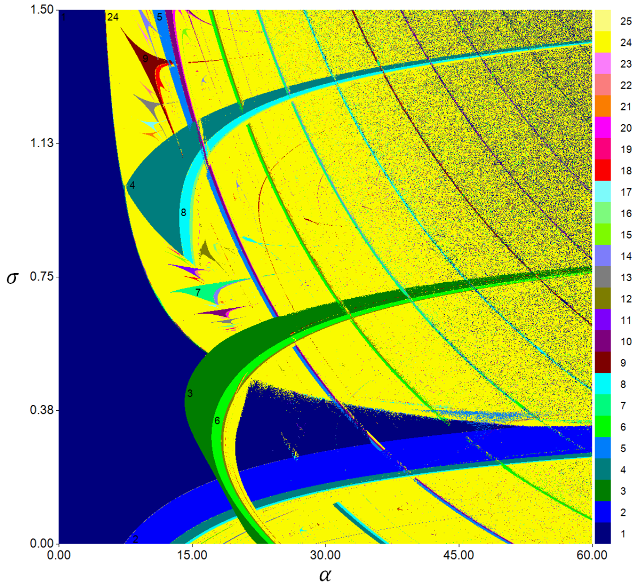

Figure 4. Two-dimensional bifurcation diagram that captures the behavior of a dynamical system at a 1:4 resonance point. The bifurcation diagram is plotted with respect to the (α, σ) parameters and illustrates the different regions of the parameter space where the system exhibits different types of behavior, such as periodic oscillations, chaos, and stability.

4. Conclusions

In conclusion, this study highlights the importance of considering time delay factors in ecological models, particularly for local population dynamics. The findings demonstrated that the incorporation of delay factors can produce complex and diverse dynamic modes, including equilibrium, periodic oscillations, and chaotic fluctuations. Moreover, the Moran–Ricker model with time lag effectively described the dynamics of several species, indicating the relevance of delay models in understanding the population dynamics of real ecosystems. The study also emphasizes the potential for shifts in dynamic modes due to changes in population size or external factors, which has significant implications for the management and conservation of natural populations. Overall, the findings of this study have important implications for ecological research, and highlight the need for the continued development of modeling techniques that can capture the complexity of real ecosystems.

In addition to providing insights into the dynamics of the Moran–Ricker model with time delay, our study has important implications for understanding and managing real-world populations. For example, the model has been used to describe the dynamics of several species, including Zeiraphera griseana and Epinotia tedella. Our findings highlight the significance of estimating population parameters, and the potential for shifts in dynamic modes due to changes in population size or external factors. Understanding these shifts and their underlying mechanisms is crucial for predicting the responses of populations to environmental change, such as global climate change or habitat loss.

Author Contributions: Methodology, Z.E.; Software, B.L.; Validation, Z.Y. All authors have read and agreed to the published version of the manuscript.

Funding: This research was funded by Natural Science Fund of Anhui Province, grant number NO. 2008085QA09.

Conflicts of Interest: The authors declare no conflict of interest.

References

1. Lotka, A.J. *Elements of Physical Biology*; Williams & Wilkins: Philadelphia, PA, USA, 1925.
2. Volterra, V. *Variazioni e Fluttuazioni del Numero d'Individui in SPECIE Animali Conviventi*; Societá anonima tipografica Leonardo da Vinci: Città di Castello, Italy, 1927; Volume 2.

3. Holling, C.S. The functional response of predators to prey density and its role in mimicry and population regulation. *Mem. Entomol. Soc. Can.* **1965**, *97*, 5–60. [CrossRef]
4. Edelstein-Keshet, L. *Mathematical Models in Biology*; SIAM: Philadelphia, PA, USA, 2005.
5. Jang, S.R.J. Allee effects in a discrete-time host-parasitoid model. *J. Differ. Eq. Appl.* **2006**, *12*, 165–181. [CrossRef]
6. Jang, S.R.J. Discrete-time host–parasitoid models with Allee effects: Density dependence versus parasitism. *J. Differ. Eq. Appl.* **2011**, *17*, 525–539. [CrossRef]
7. Livadiotis, G.; Assas, L.; Dennis, B.; Elaydi, S.; Kwessi, E. A discrete-time host-parasitoid model with an Allee effect. *J. Biol. Dyn.* **2015**, *9*, 34–51. [CrossRef]
8. Wang, W.X.; Zhang, Y.B.; Liu, C.Z. Analysis of a discrete-time predator-prey system with Allee effect. *Ecol. Complex.* **2011**, *8*, 81–85. [CrossRef]
9. Naik, P.A.; Eskandari, Z.; Yavuz, M.; Zu, J. Complex dynamics of a discrete-time Bazykin-Berezovskaya prey-predator model with a strong Allee effect. *J. Comput. Appl. Math.* **2022**, *413*, 114401. [CrossRef]
10. Neverova, G.P.; Yarovenko, I.P.; Frisman, E.Y. Dynamics of populations with delayed density dependent birth rate regulation. *Ecol. Model.* **2016**, *340*, 64–73. [CrossRef]
11. Moran, P.A.P. Some remarks on animal population dynamics. *Biometrics* **1950**, *6*, 250–258. [CrossRef]
12. Nedorezov, L.V.; Sadykova, D.L. Green oak leaf roller moth dynamics: An application of discrete time mathematical models. *Ecol. Model.* **2008**, *212*, 162–170. [CrossRef]
13. Nedorezov, L.V. Analysis of pine looper population dynamics using discrete time mathematical models. *Mat. Biol. Bioinformatika* **2010**, *5*, 114–123. [CrossRef]
14. Turchin, P. Complex population dynamics. In *Complex Population Dynamics*; Princeton University Press: Princeton, NJ, USA, 2013.
15. Zhdanova, O.L.; Frisman, E.Y. Manifestation of multimodality in a simple ecological-genetic model of population evolution. *Russ. J. Genet.* **2016**, *52*, 868–876. [CrossRef]
16. Li, B.; Zhang, Y.; Li, X.; Eskandari, Z.; He, Q. Bifurcation analysis and complex dynamics of a Kopel triopoly model. *J. Comput. Appl. Math.* **2023**, *426*, 115089. [CrossRef]
17. Eskandari, Z.; Avazzadeh, Z.; Khoshsiar Ghaziani, R.; Li, B. Dynamics and bifurcations of a discrete-time Lotka–Volterra model using nonstandard finite difference discretization method. *Math. Methods Appl. Sci.* **2022**. [CrossRef]
18. Naik, P.A.; Eskandari, Z.; Madzvamuse, A.; Avazzadeh, Z.; Zu, J. Complex dynamics of a discrete-time seasonally forced SIR epidemic model. *Math. Methods Appl. Sci.* **2022**. [CrossRef]
19. Eskandari, Z.; Khoshsiar Ghaziani, R.; Avazzadeh, Z. Bifurcations of a discrete-time SIR epidemic model with logistic growth of the susceptible individuals. *Int. J. Biomath.* **2022**, *16*, 2250120. [CrossRef]
20. Li, B.; Eskandari, Z.; Avazzadeh, Z. Dynamical Behaviors of an SIR Epidemic Model with Discrete Time. *Fractal Fract.* **2022**, *6*, 659. [CrossRef]
21. Kuznetsov, Y.A. *Elements of Applied Bifurcation Theory*; Springer: Berlin/Heidelberg, Germany, 2013; Volume 112.
22. Kuznetsov, Y.A.; Meijer, H.G. Numerical normal forms for codim 2 bifurcations of fixed points with at most two critical eigenvalues. *SIAM J. Sci. Comput.* **2005**, *26*, 1932–1954. [CrossRef]
23. Kuznetsov, Y.A.; Meijer, H.G. *Numerical Bifurcation Analysis of Maps: From Theory to Software*; Cambridge University Press: Cambridge, UK, 2019.
24. Govaerts, W.; Ghaziani, R.K.; Kuznetsov, Y.A.; Meijer, H.G. Numerical methods for two-parameter local bifurcation analysis of maps. *SIAM J. Sci. Comput.* **2007**, *29*, 2644–2667. [CrossRef]